ISIJ International, Vol. 44 (2004), No. 12, pp. 2100–2104

Reduction Behavior of FeO Compact Including Molten Slag

Masashi NAKAMOTO, Hideki ONO-NAKAZATO,[1)] Hirotoshi KAWABATA,[1)] Tateo USUI[1)] and Toshihiro TANAKA[1)]

Graduate Student, Osaka University, 2-1 Yamadaoka, Suita, Osaka 565-0871 Japan.
1) Graduate School of Engineering, Osaka University, 2-1 Yamadaoka, Suita, Osaka 565-0871 Japan.

(Received on May 6, 2004; accepted in final form on October 8, 2004)

FeO compact including molten slag was reduced with H_2 at 1 500 K, and the effect of the slag penetration in the reducibility was investigated. Two kinds of molten slag, which coexist with solid FeO, in FeO–SiO_2–CaO systems were used and the influence of the physical properties of molten slag, especially viscosity, on the reducibility was investigated. The penetrations of the molten slag with a low viscosity to the grain boundaries produce the spaces, which are useful as the pass of the reduction gas, in the interspaces between the grains. Then, the reduction rate of the FeO compact containing molten slag with a low viscosity is higher than that of the FeO compact containing molten slag with a high viscosity.

KEY WORDS: ironmaking; iron oxide; reducibility; molten slag; penetration; viscosity.

1. Introduction

The innovation of ironmaking process is required for solving energy and environment problems all over the world, such as the reduction of CO_2 emission and the decrease of quality of iron ores, *etc.* In Japan, the project on the innovation of ironmaking process by blast furnace for the purpose of halving energy consumption and minimizing environmental influence has been promoted by Ministry of Education, Culture, Sports, Science, and Technology.[1)]

In this project, the studies of lowering the melting temperature of slag have been conducted by some researchers.[2–8)] It is recognized commonly that the concentration of FeO in iron ore and sinter influences the melting behavior of slag. Hasegawa and Iwase[2)] indicate that the better understanding of the reduction of iron ore is important in the "softening and melting zone" of blast furnaces. Hino *et al.*[3)] report that the dripping behavior of the primary melt in the cohesive zone of blast furnace is affected by FeO content. On the other hand, Naito[9)] indicates that the reducibility of iron ore at high temperature, especially from 1 273 K to the temperature at the top of the cohesive zone, is significant for blast furnace process. The reduction behavior changes greatly in this temperature range because a molten slag closes the pores in iron ore. Therefore, many researches[10–14)] on the reducibility of iron ore and sinter have been carried out at the temperature which molten slag exists. However, the effect of the pore blockage on the reducibility is not so clear since most of reduction experiments have been conducted using the sinter or pellet, which have heterogeneous structures and phases, and the pore blockages were accompanied by phase changes when the slag in the sinter or pellet melted.

We investigated the effect of pore blockage on the reduction behavior of the FeO compact containing the molten FeO–SiO_2 slag, which coexists with solid FeO.[15)] In this system, the phase changes don't occur because the molten FeO–SiO_2 slag and solid FeO coexist in equilibrium state. We found the reduction rate of the FeO compact was decreased by the prevention of the diffusion of reducing gas due to the pore blockage by the penetration of the molten slag. But we should also examine the effect of other slag components on the reducibility because the sinter and iron ore containing various oxides are used in a conventional blast furnace.

In the present study, we investigated the effect of pore blockage on the reduction behavior of the FeO compact containing molten slag in FeO–SiO_2–CaO system. Two types of slag, FeO–SiO_2 slag (FS) and FeO–SiO_2–CaO slag (FSC), which coexist with solid FeO in equilibrium state, were used (see **Fig. 1**).[16)] Penetration experiment was conducted in order to examine the state of pore blockage, which affects the reduction behavior. Then, the reducibility of the FeO compact containing the slag was evaluated through the difference of the physical properties of molten slag.

2. Experimental

2.1. Reduction Experiment

2.1.1. Slag Preparation

The slag was prepared from the reagent grade $CaCO_3$, Fe, Fe_2O_3 and SiO_2. $CaCO_3$ powder was calcined for 5 h at 1 273 K to make CaO. The mixed powder, which corresponds to a given composition of molten slag shown in **Table 1**, was melted in an Fe crucible for 1 h under argon atmosphere (400 cc/min (s.t.p.)). The molten slag coexists with solid FeO at 1 500 K, as shown in Fig. 1.[16)] These oxides are equilibrated with metallic iron. Then, the molten slag in the Fe crucible was quenched in iced water, and the

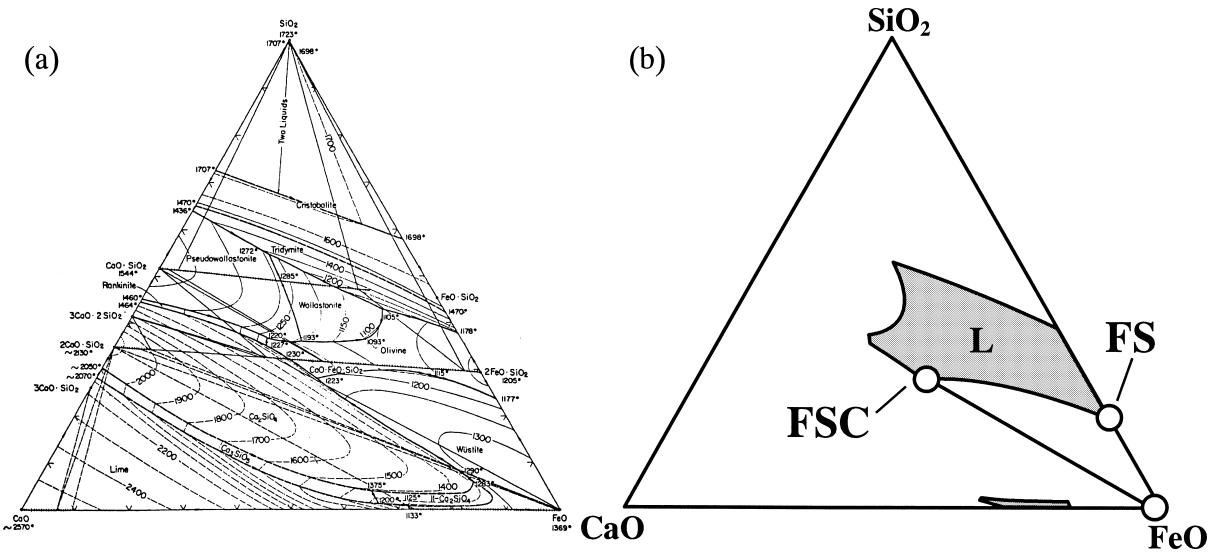

Fig. 1. Phase diagrams for FeO–SiO_2–CaO system. (a) Given by Muan and Osborn[16] and (b) at 1 500 K.

Table 1. Chemical composition of slag.

	FS	FSC
FeO	81.1	42
SiO_2	18.9	27.5
CaO		30.5

(mass%)

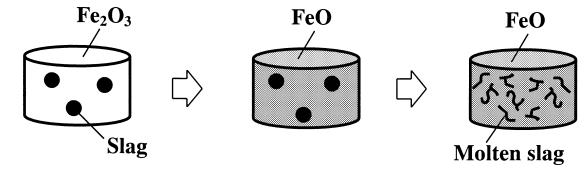

(a) Fe_2O_3 compact with slag grains (b) FeO compact with slag grains at 1273 K in 60%H_2-40%CO_2 (c) FeO compact with molten slag at 1500 K in 60%H_2-40%CO_2 for 30min

Fig. 2. Schematic illustration of procedure for sample preparation.

slag was crushed and sieved to 0.3–1 mm.

2.1.2 Sample Preparation

Schematic illustration of procedure for sample preparation is shown in **Fig. 2**. The Fe_2O_3 powder, heated at 1 273 K for 3 h, was sieved to under 45 μm. The Fe_2O_3 compact added with the slag grains produced as mentioned above was prepared by mixing weighed quantities of them, as shown in **Table 2**, and by pressing the mixture at 100 MPa for 3 min in a cylindrical mould (see Fig. 2 (a)). The compact is a cylinder of about 15 mm in diameter and 7 mm in height. The sample was reduced to FeO at 1 273 K in fixed 60%H_2–40%CO_2 gas mixture (see Fig. 2 (b)). The phases of the sample cooled under argon flushing (400 cc/min (s.t.p.)) were analyzed by an X-ray diffraction (XRD). **Figure 3** shows the XRD pattern for the sample without slag. As expected, it is confirmed that all of the XRD peaks correspond to FeO. Although the XRD peaks of Fe are also found, the intensity of these peaks is weak. The typical cross section of the sample observed by a laser-microscope is shown in **Fig. 4**. White part is FeO, and it is predicted black part is pore. The interspaces among grains

Table 2. Composition of samples, Fe_2O_3 and slag grain (FS or FSC), and the estimated FeO: molten slag (FS or FSC) at 1 500 K.

Fe_2O_3	:	Slag	FeO	:	Molten slag
100	:	0	100	:	0
99.9	:	0.1	99.4	:	0.6
99.8	:	0.2	98.5	:	1.5
99.6	:	0.4	97.4	:	2.6
99.1	:	0.9	94.4	:	5.6

(mass%)

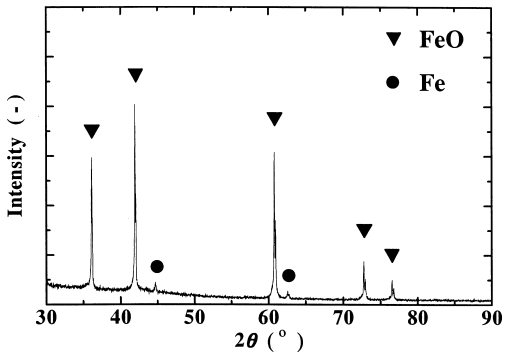

Fig. 3. X-ray diffraction pattern for the sample without slag.

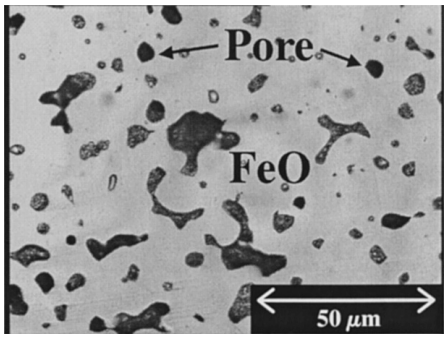

Fig. 4. Typical cross section of the sample.

and grain boundaries cannot be identified in Fig. 4. It is difficult to consider that the interspaces among grains and grain boundaries disappear in the sintering by taking ac-

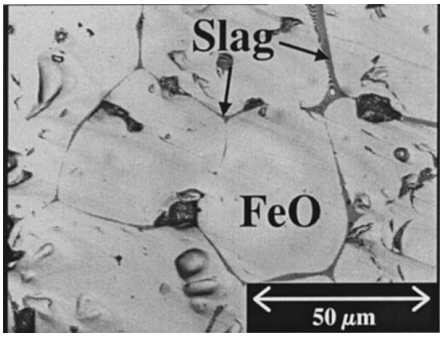

Fig. 5. Cross section of the sample containing slag.

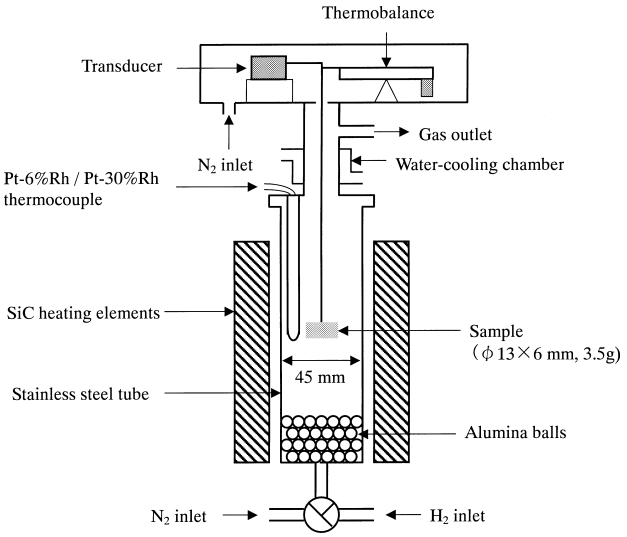

Fig. 6. Schematic cross section of experimental apparatus.

count of the temperature and the heating time in sample preparation. Accordingly, it is considered that these parts were closed at the polishing due to the softness of sample. The sample in Fig. 2(b) was heated up to 1500 K at a heating rate of 10 K/min and was kept under the same condition with an equilibration time of 30 min (see Fig. 2(c)). Assuming that Fe_2O_3 transforms FeO under this condition, the amount of molten slag is estimated as 0, 0.6, 1.5, 2.6, 5.4 mass% as tabulated in Table 2. Then, the sample was cooled under argon flushing (400 cc/min (s.t.p.)). The XRD pattern and the cross-sectional view of the sample without slag are the same as those of the sample in Fig. 2(b). On the other hand, slag can be observed in the case of the sample containing slag, as shown in **Fig. 5**. It is found that this slag exists in the interspaces among grains and grain boundaries because the size of the region surrounded by this slag is similar to Fe_2O_3 grain size (<45 μm) used for the production of compact.

2.1.3. Procedure

The experimental setup used for reduction experiment is illustrated in **Fig. 6**. After the sample was heated up to 1 500 K at a heating rate of 10 K/min in N_2 flow (400 cc/min (s.t.p.)), the sample was kept for an equilibration time of 30 min. The reduction was started by introducing hydrogen (1 000 cc/min (s.t.p.)). In order to assess the kinetics of reduction reaction, thermogravimetric analysis was performed using a thermobalance. The sensitivity of the balance was in the order of 2 μg.

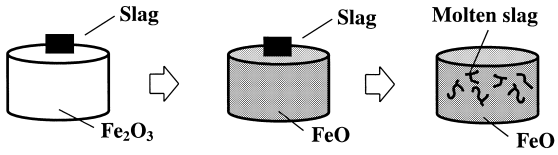

(a) Slag tablet on Fe_2O_3 compact (b) Slag tablet on FeO compact at 1273 K in 60%H_2-40%CO_2 (c) Molten slag penetrates to FeO compact at 1500 K in 60%H_2-40%CO_2 for 30min

Fig. 7. Schematic illustration of penetration experiment.

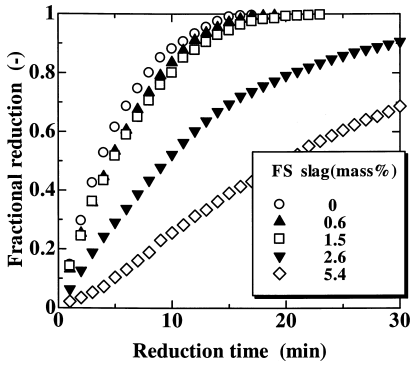

Fig. 8. Reduction behavior of FeO compact with molten slag FS. 100% H_2, flow rate: 1 000 cc/min (s.t.p.), temperature: 1 500 K.

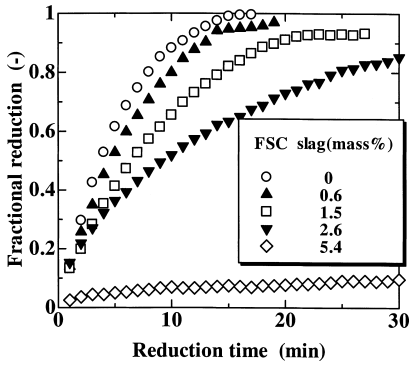

Fig. 9. Reduction behavior of FeO compact with molten slag FSC. 100% H_2, flow rate: 1 000 cc/min (s.t.p.), temperature: 1 500 K.

2.2. Penetration Experiment

Schematic illustration of penetration experiment is shown in **Fig. 7**. Slag FS or FSC tablet of 0.04 g was placed on the Fe_2O_3 compact of 4 g (see Fig. 7(a)). Both of the slag and the compact were prepared as same as the method shown in Sec. 2.1.1. The sample was reduced to FeO at 1 273 K in 60%H_2–40%CO_2 gas mixture (see Fig. 7(b)). It was heated up to 1 500 K at a heating rate of 10 K/min and was kept in 60%H_2–40%CO_2 gas mixture for 30 min (see Fig. 7(c)). Here, the slag tablet melted, and the molten slag penetrated to the bulk of the FeO compact. The cross sections of the compact were observed by a laser-microscope.

3. Results and Discussion

3.1. Reduction Experiment

Figures 8 and **9** show the reduction curves obtained in the reduction experiments with samples containing slag FS

and FSC, respectively. The reduction rate of both samples decreases as the amount of slag increases. These decreases of the reduction rate are explained from the pore blockage due to the penetration phenomena of molten slag.[15] The reduction behaviors of two samples are different, and the reduction rate of the sample with slag FSC is lower than that of the sample with slag FS. This difference of the reduction behaviors is considered to be attributable to the state of the penetration, *i.e.* pore blockage, of molten slag since the two types of molten slag coexist with solid FeO, and don't react with other phases. However, it is difficult to examine the state of penetration of the sample used for the reduction experiment because of the random distribution of slag grains in the sample. Then, the penetration experiments were carried out.

3.2. Penetration Experiment

The cross-sectional views of the samples, to which slag FS and FSC penetrate, are shown in **Figs. 10** and **11**, respectively. The slag exists in the interspaces among the grains and in the grain boundary in both samples. However, there is no FSC slag in the bottom part of sample. Moreover, the area of slag FSC exists in the interspaces among the grains is larger than that of slag FS. On the contrary, the area of the slag FSC exists in the grain boundary is less than that of slag FS. These are considered to be due to the difference of penetration behavior between slag FS and slag FSC.

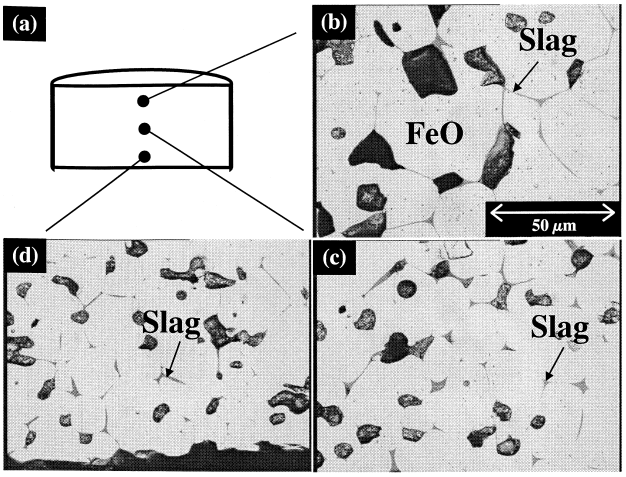

Fig. 10. Microscopic observation of the sample, to which molten slag FS penetrates, in penetration experiment. (a) Schematic representation of sample, (b) image at the top part, (c) image at the middle part, (d) image at the bottom part.

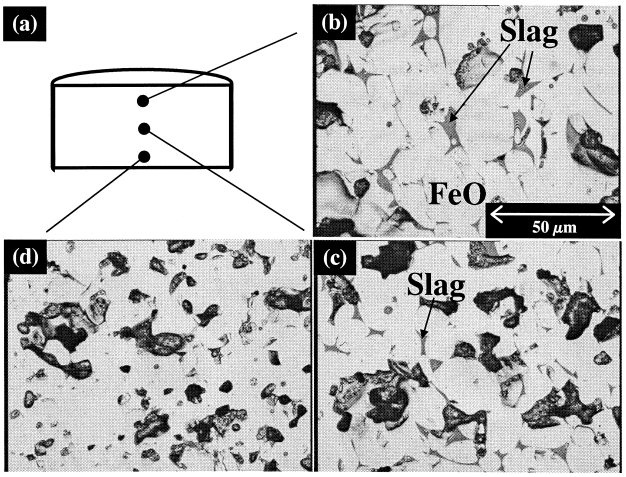

Fig. 11. Microscopic observation of the sample, to which molten slag FSC penetrates, in penetration experiment. (a) Schematic representation of sample, (b) image at the top part, (c) image at the middle part, (d) image at the bottom part.

The equation of penetration is expressed as follows[17]:

$$\frac{d(l^2)}{dt} = \frac{K_r \gamma_{LV} \cos\theta}{\eta_L} \quad \text{.....(1)}$$

where l is the penetration length of the liquid, $K_r = /(2k^2)$, r is the average pore radius, k is a constant introduced to account for the tortuosity of the capillary pores, γ_{LV} is the surface tension of the liquid, θ is the contact angle between the liquid and solid, η_L is the viscosity of the liquid and t is the time of penetration. Since K_r is the coefficient which is related to the structure of FeO compact and all compacts are produced by the same method, K_r is constant and the penetration behavior is dependent on the physical properties of molten slag, such as the contact angle between molten slag and FeO, the surface tension and viscosity of the molten slag.

The contact angle between molten slag FS and FeO is considered to be similar to that between molten slag FSC and FeO because the wettability of the two types of molten slag, which coexist with solid FeO, to solid FeO is very good. The surface tension[18,19] and viscosity[20] for $FeO–SiO_2–CaO$ system are shown in **Figs. 12** and **13**, respectively. The composition dependence of viscosity is much larger than that of surface tension. Therefore, the penetration behavior of molten slag is mainly dependent on the viscosity.

However, to our knowledge, there are no data of the viscosity under the present experimental composition and temperature. Then, we estimated the viscosity of molten slag by using our viscosity model.[5] The calculated results of the viscosity for $FeO–SiO_2–CaO$ system are shown in **Fig. 14**. Since the viscosity of molten slag FSC is about four times as high as that of molten slag FS, the penetration rate of slag FSC is much slower than that of slag FS. As shown in

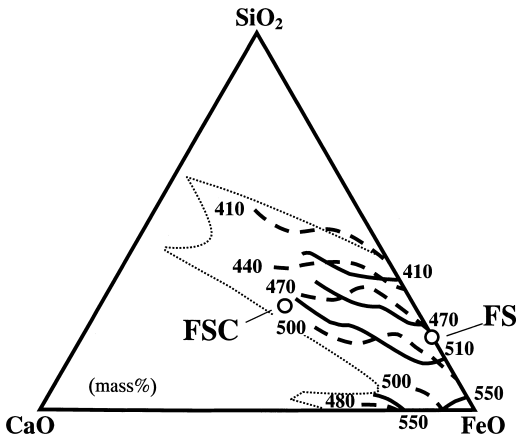

Fig. 12. Surface tension γ_L (mN/m) for $FeO–SiO_2–CaO$ system at 1 673 K. Solid line: Kozakevitch,[18] broken line: Kawai *et al.*,[19] dotted line: liquidus at 1 673 K.

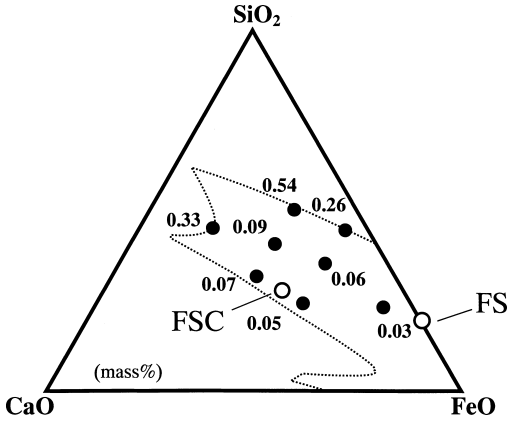

Fig. 13. Viscosity η_L (Pa·s) for FeO–SiO_2–CaO system at 1 673 K. Closed circle: Seetharaman *et al.*,[20] dotted line: liquidus at 1 673 K.

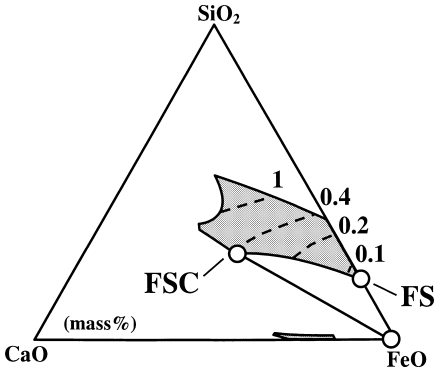

Fig. 14. Calculated viscosity η_L (Pa·s) for FeO–SiO_2–CaO system at 1 500 K.

Fig. 8, molten slag FSC does not permeate to the bottom part of sample, which gives the evidence for slow penetration. It is also guessed that the molten slag FSC with a high viscosity can penetrate to not the grain boundaries with slight spaces but the interspaces between the grains, preferentially. The interspaces between grains closed by molten slag prevent the supply of the reduction gas to the bulk of FeO compact. On the other hand, the molten slag FS with a low viscosity penetrates not only the interspaces between the grains but also the grain boundaries. The penetrations of the molten slag to the grain boundaries produce the spaces in the interspaces between the grains. These spaces are useful as the pass of the reduction gas. Therefore, the decrease of the reduction rate of the FeO compact containing slag FS decreases is less than that of the FeO compact containing slag FSC.

4. Conclusions

The reduction experiments of FeO compact including molten slag with H_2 gas at 1 500 K have been conducted by using the two types of molten slag for FeO–SiO_2 system (FS) and FeO–SiO_2–CaO system (FSC), which coexist with solid FeO, and the penetration experiments have been also conducted. The results obtained are summarized as follows:

(1) The reduction rate of the FeO compact containing molten salg decreases with increasing the amount of molten slag regardless of the type of the molten slag.

(2) The molten slag FSC with a high viscosity permeates the interspaces among the grains preferentially, and the molten slag FS with a low viscosity permeates to not only the interspaces among the grains but also the grain boundaries.

(3) Since the penetrations of the molten slag FS with a low viscosity to the grain boundaries produce the spaces, which are useful as the pass of the reduction gas, in the interspaces between the grains, the reduction rate of the FeO compact with molten slag FS is higher than that of the FeO compact with molten slag FSC with a high viscosity.

REFERENCES

1) K. Ishii and J. Yagi: *Tetsu-to-Hagané*, **87** (2001), 207.
2) M. Hasegawa and M. Iwase: Proc. of Science and Technology of Innovative Ironmaking for Aiming at Energy Half Consumption, ISIJ, Tokyo, (2003), 149.
3) M. Hino, T. Nagasaka, A. Katsumata, K. Higuchi, K. Yamaguchi and N. Konno: *Metall. Mater. Trans. B*, **30B** (1999), 671.
4) K. Nagata, T. Murakami and I. Seki: Proc. of Science and Technology of Innovative Ironmaking for Aiming at Energy Half Consumption, ISIJ, Tokyo, (2003), 135.
5) T. Tanaka, M. Nakamoto, J. Lee and T. Usui: Proc. of Science and Technology of Innovative Ironmaking for Aiming at Energy Half Consumption, ISIJ, Tokyo, (2003), 161.
6) T. Usui, H. Kawabata, H. Ono-Nakazato, M. Nakamoto, K. Tanaka and N. Goto: Proc. of Science and Technology of Innovative Ironmaking for Aiming at Energy Half Consumption, ISIJ, Tokyo, (2003), 165.
7) T. Matsui, N. Ishiwata, Y. Hara and K. Takeda: Proc. of Science and Technology of Innovative Ironmaking for Aiming at Energy Half Consumption, ISIJ, Tokyo, (2003), 177.
8) S. Inaba: Proc. of Science and Technology of Innovative Ironmaking for Aiming at Energy Half Consumption, ISIJ, Tokyo, (2003), 187.
9) M. Naito: *CAMP-ISIJ*, **10** (1997), 743.
10) M. Naito, A. Okamoto, K. Ono and Y. Hayashi: *Tetsu-to-Hagané*, **71** (1985), 49.
11) A. Okamoto, M. Naito, K. Ono and Y. Hayashi: *Tetsu-to-Hagané*, **72** (1986), 3.
12) Y. Hosotani, N. Konno, K. Yamaguchi, T. Orimoto and T. Inazumi: *ISIJ Int.*, **36** (1996), 1439.
13) K. Yamaguchi, K. Higuchi, Y. Hosotani, A. Ohshio and S. Kasama: *Tetsu-to-Hagané*, **84** (1998), 14.
14) K. Yamaguchi: *Tetsu-to-Hagané*, **87** (2001), 335.
15) M. Nakamoto, H. Ono-Nakazato, H. Kawabata and T. Usui: *Tetsu-to-Hagané*, **90** (2004), 1.
16) A. Muan and E. F. Osborn: Phase Equilibria among Oxides in Steelmaking, Addison-Wesley Publishing, Inc., MA, (1965), 54, 113.
17) R. E. Ayala, E. Z. Casassa and G. D. Parfitt: *Powder Technol.*, **51** (1987), 3.
18) P. Kozakevitch: *Rev. Metall., Cah. Inf. Tech.,* **46** (1949), 572.
19) Y. Kawai, K. Mori, Y. Shiraishi and N. Yamada: *Tetsu-to-Hagané*, **62** (1976), 53.
20) S. Seetharaman, D. Sichen and F. -Z. Ji: *Metall. Mater. Trans. B*, **31B** (2000), 105.